Disclosure of Double Exchange Bias Effect in Chromium (III) Oxide Nanoparticles

Natalia Rinaldi-Montes[1,2], Pedro Gorria[3], Antonio B. Fuertes[4], David Martínez-Blanco[5], Luca Olivi[6], Inés Puente-Orench[7], Javier Alonso[2,8], Manh-Huong Phan[2], Hariharan Srikanth[2], Xavi Marti[9], and Jesús A. Blanco[1]

[1]Departamento de Física, Universidad de Oviedo, Oviedo 33007, Spain
[2]Department of Physics, University of South Florida, Tampa, 33620 USA
[3]Departamento de Física e Instituto Universitario de Tecnología Industrial de Asturias, Escuela Politécnica de Ingeniería, Universidad de Oviedo, Gijón 33203, Spain
[4]Instituto Nacional del Carbón, Consejo Superior de Investigaciones Científicas, Oviedo 33080, Spain
[5]Servicios Científico-Técnicos, Universidad de Oviedo, Oviedo 33006, Spain
[6]Elettra-Sincrotrone Trieste S.C.p.A., Trieste 34149, Italy
[7]Institut Laue-Langevin, Grenoble 38042, France
[8]BCMaterials, Parque Tecnológico de Bizkaia, Derio 48160, Spain
[9]Institute of Physics, Czech Academy of Sciences, Prague 162 53, Czech Republic

In the last decade, the renewed interest in antiferromagnetic (AF) magnetoelectric (ME) materials has been driven by the challenging multifunctionality of spintronic devices. One of the most ambitious goals is to build exchange-biased ferromagnetic/AF junctions with electric field-controlled properties. In this context, the understanding of the modifications that size reduction induces in the magnetic properties of a material being both AF and ME holds the key to control the magnetic coupling at the interface. Here, we show that the spin arrangement in chromium (III) oxide core/shell nanoparticles changes significantly as a function of the radial distance from the nanoparticle center. While the nanoparticle core retains an AF structure, magnetic moments located on a thin surface shell are in a disordered spin-glass (SG)-like state. In addition, canted spins develop at the boundary of the ME AF core. These spins, which mediate a moderate AF/SG exchange coupling at low temperature, are exchange coupled to the AF core, thus giving rise to a lower yet more robust exchange bias effect, which persists up to the Néel temperature of the AF core.

Index Terms— **Antiferromagnetism, exchange bias (EB), magnetic nanoparticles, magnetoelectric effect.**

I. Introduction

As far back as 1894, the linear magnetoelectric (ME) effect was first predicted by Curie [1] and theoretically formulated in 1958 by Landau and Lifshitz [2]. In the following year, Dzyaloshinskii [3] derived the expressions for a linear ME coupling in chromium (III) oxide (Cr_2O_3) based on symmetry arguments. By that time, electronic industry was already exploiting the technological potential of controlling the electric and magnetic polarization properties of a material by complementary fields [4]. Nowadays, more than 50 years later, the new generation of spintronic devices, including magnetoresistive random access memories (MRAMs) [5] and voltage-driven tunnel junctions [6], has brought multiferroic ME materials back to the forefront of materials science research [7]. Alternatively, antiferromagnetic (AF) materials are also being reviewed as potential candidates for spintronic applications [8], [9]. Moreover, it has been proposed that the use of an ME antiferromagnet in contact with a ferromagnet as a way to control the ferromagnetic (FM) state [10]. It is well known that AF/FM heterostructures exhibit an interfacial magnetic coupling that gives rise to an exchange bias (EB) effect. This manifests as a horizontal shift of the FM hysteresis loop when the system is cooled below the Néel temperature (T_N) of the AF component in the presence of an applied magnetic field (H_{cool}) [11]. Furthermore, when the antiferromagnet is also ME, the interface coupling could be tuned by the application of an electric field [10]. Thus, EB can be electric-field-controlled in a reversible way. Nevertheless, this only develops far below room temperature due to the fact that, in the previously reported systems, either the EB is rather weak or the AF order sets at low temperature [12], [13]. However, suitable materials that can operate at or near ambient temperatures are still rather scarce [14], [15]. In this context, Cr_2O_3 emerges as a promising candidate, since it becomes ME below its AF ordering temperature of $T_N \sim 307$ K. In particular, Borisov *et al.* [16] succeeded in creating a novel ME-based switching mechanism for the EB field in a Cr_2O_3–Co/Pt multilayered sensor. In order to overcome the grand challenge for pushing the miniaturization limits of EB-based spintronics devices, it is of paramount importance to understand and control the changes that size reduction induces in the magnetic properties of an antiferromagnet.

Numerous experimental and theoretical investigations have been performed so far to elucidate this issue in a number of AF NPs (e.g., NiO, CuO, CoO, Co_3O_4, and Cr_2O_3) [17]–[21].

Manuscript received May 5, 2016; revised June 6, 2016; accepted June 28, 2016. Date of publication July 7, 2016; date of current version December 20, 2016. Corresponding author: N. Rinaldi-Montes (e-mail: nataliarin@gmail.com).

Color versions of one or more of the figures in this paper are available online at http://ieeexplore.ieee.org.

Digital Object Identifier 10.1109/TMAG.2016.2587158

It is now generally accepted that each NP can be considered as a core/shell EB system, where a weak FM or spin-glass (SG) shell is exchange coupled to a core that retains the original AF order of the bulk material [22]. However, in a recent theoretical study, Belashchenko [23] used symmetry arguments to show that an ME antiferromagnet develops finite equilibrium magnetization at the surface. Interestingly, the EB arising from this surface magnetization is an equilibrium property of the system.

In this paper, we show that the magnetic structure of Cr_2O_3 NPs has an important role for understanding the phenomenology of the EB effect. Our findings suggest that: 1) the NP core retains the AF structure of Cr_2O_3; 2) spins located on the NP surface are magnetically disordered and experience an SG-like freezing at low temperature (25 K); and 3) canted spins located at the core/shell interface are not only exchange coupled to the AF core at $25 < T < 270$ K but also mediate the core/shell coupling at $T < 25$ K.

II. Experiment

Cr_2O_3 NPs were fabricated using a template-assisted method [24]. Mesoporous silica xerogel was impregnated with a chromium nitrate solution and calcined in air at 400 °C. The subsequent removal of the silica framework by NaOH etching produced highly crystalline Cr_2O_3 NPs. Both the high-resolution transmission electron microscopy (HRTEM) images and the selected-area electron diffraction (SAED) patterns were obtained under a JEOL-JEM-2100F microscope operating at 200 kV.

The neutron powder diffraction (ND) measurements were carried out at the Institut Laue-Langevin (Grenoble, France) on a two-axis powder diffractometer (D1B instrument) equipped with a high efficiency position sensitive detector. ND patterns in a 2θ angular range of $1° - 128°$ were collected at a neutron wavelength of $\lambda = 2.52$ Å. A double-walled vanadium cylinder sample holder was used to reduce neutron absorption. $Al_2Ca_3F_{14}Na_2$ and Si standards were measured so as to account for instrumental resolution. Analysis of the ND data was performed using the FullProf suite package [25].

The dc magnetic properties of the Cr_2O_3 NPs were studied using a Quantum Design PPMS-14T magnetometer equipped with the VSM option. The magnetization versus temperature measurements were performed under zero-field-cooling (ZFC) and field-cooling (FC) conditions under an applied magnetic field of 100 Oe. Hysteresis loops were recorded between −60 and 60 kOe after FC ($H_{cool} = 10$ kOe) protocol at different temperatures ranging from 2 to 300 K.

III. Results and Discussion

The obtained Cr_2O_3 NPs [Fig. 1(a)] present an average diameter of 17(3) nm, as derived from the lognormal distribution fit of the size histogram created from multiple HRTEM images. The diffraction rings observed in the SAED pattern in Fig. 1(b) can be indexed according to the same corundum-type crystal structure as hematite (α-Fe_2O_3), described in terms of a hexagonal unit cell for a $R\bar{3}c$ space group (No. 167). Both the lattice parameters, $a = 4.951(1)$ Å and $c = 13.590(1)$ Å, and the adjustable atomic positions, $z_{Cr} = 0.346(1)$ and $x_O = 0.309(1)$, coincide with those reported for bulk Cr_2O_3 [26].

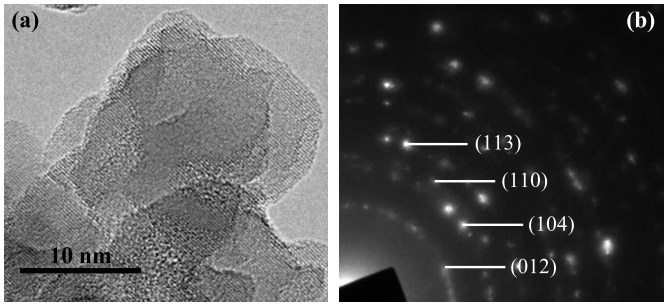

Fig. 1. (a) HRTEM image of Cr_2O_3 NPs. (b) SAED pattern showing diffraction rings corresponding to a *R-3c* crystal structure.

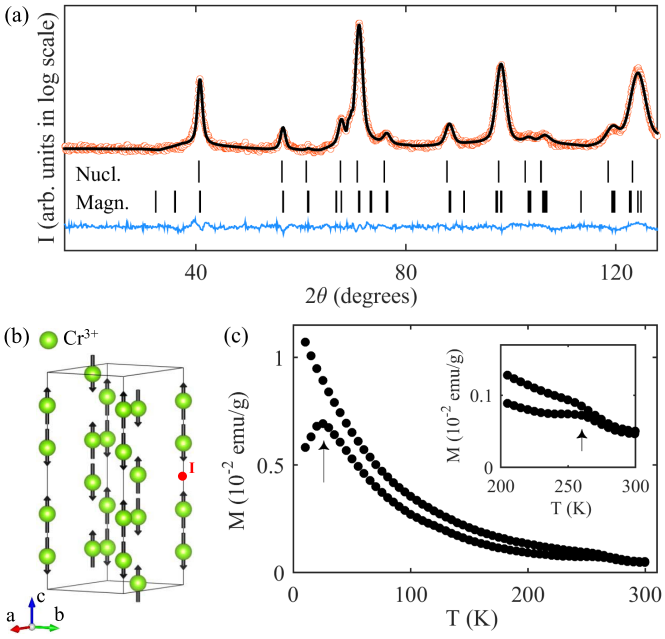

Fig. 2. (a) ND pattern in logarithmic vertical scale at $T = 100$ K. Vertical marks: position of the allowed Bragg reflections. (b) Magnetic structure of Cr_2O_3. The position I marks a center of space-inversion symmetry. (c) ZFC and FC magnetization curves measured under an applied magnetic field of 100 Oe. Inset: enlarged view of the region where T_N is located.

Information about the spin arrangement inside the Cr_2O_3 NPs is provided by neutron diffraction. The full-profile fitting of the ND pattern recorded at $T = 100$ K [Fig. 2(a)] reveals that the crystallographic unit cell coincides with the same corundum-like structure as derived from SAED measurements. In addition, the AF structure of Cr_2O_3 can be described in terms of a magnetic propagation vector $k = (0, 0, 0)$ referred to the crystallographic unit cell [Fig. 2(b)], where the magnetic moments are oriented along the c axis following the $\{+-+-\}$ sequence [26]. On the other hand, the value of μ decreases substantially to 1.82(3) μ_B. Besides, the coherent magnetic domain size (D_m) is significantly reduced with respect to that of the crystallographic ones (D_n), both being obtained from the full-profile fitting of the 100-K ND pattern. While D_n coincides with the previously estimated value from the HRTEM size distribution [17(1) nm], D_m is around 4 nm

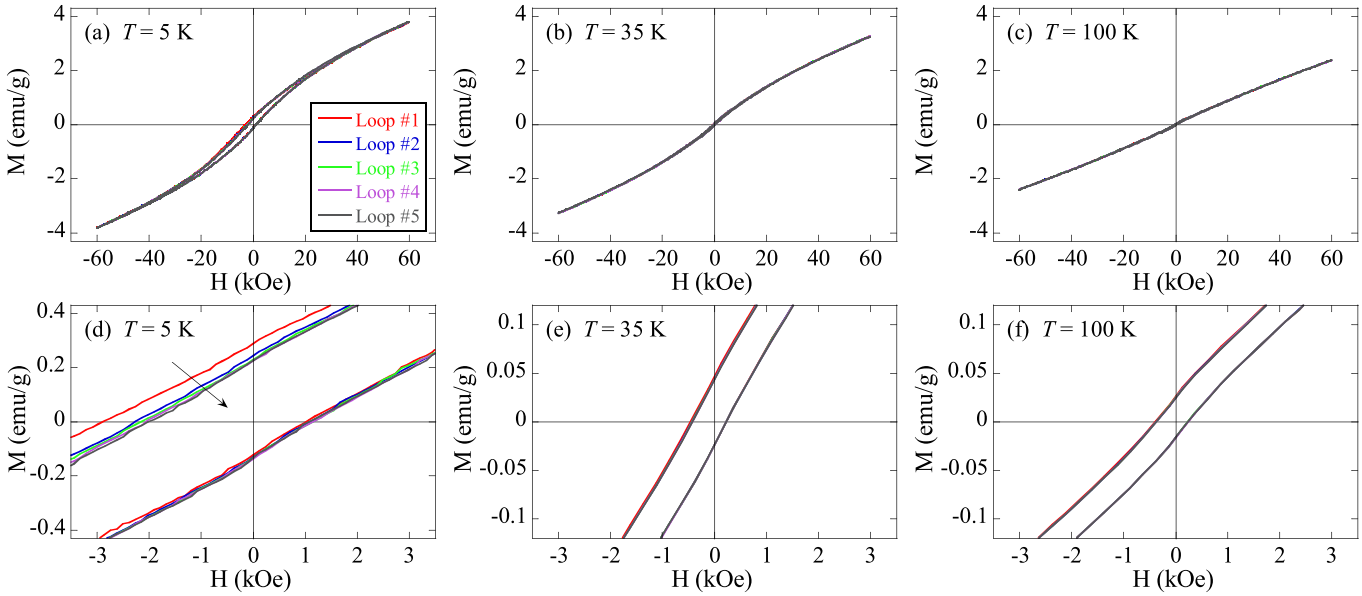

Fig. 3. (a)–(c) Magnetic hysteresis loops measured at $T = 5$, 35, and 100 K under FC ($H_{cool} = 10$ kOe) conditions after successive field cycling. (d)–(f) Enlarged view of the central region of the loops.

smaller [13(1) nm]. The simultaneous decrease of μ and D_m has been extensively observed in fine-particle systems and attributed to the presence of a magnetically disordered shell at the surface of the NPs as a consequence of their lower atomic coordination number [27]. It is worth noting that the existence of canted antiferromagnetism in bulk Cr_2O_3 is forbidden by symmetry restrictions (space-inversion and time-reversal symmetry). However, the lattice periodicity breaking at the NP surface may overcome the aforementioned symmetry conditions.

A general picture of the magnetic response of the Cr_2O_3 NPs can be drawn starting from the ZFC, $M_{ZFC}(T)$, and FC, $M_{FC}(T)$, curves recorded under an applied field (H) of 100 Oe [Fig. 2(c)]. $M_{FC}(T)$ shows a continuous increase as temperature is reduced. On the other hand, $M_{ZFC}(T)$ exhibits two peaks at low (∼25 K) and high (∼270 K) temperatures. Remarkably, this latter temperature also determines the onset of the splitting between M_{ZFC} and M_{FC}, which becomes larger on further cooling the system [Fig. 2(c) (inset)]. Based on the ND results, the high-temperature maximum seems to correspond to the T_N of AF Cr_2O_3, while the low-temperature one may be assigned to the SG-like freezing of magnetically disordered surface spins. According to this, each NP could be described as consisting of a 13 nm-core that retains the AF order of bulk Cr_2O_3, characterized by a Néel temperature of $T_N \sim 270$ K, and a 2 nm-thick surface shell (see ND results) where disordered magnetic moments freeze in an SG-like state below $T_g \sim 25$ K. However, a simplistic core/shell model cannot account for the splitting of the M_{ZFC} and M_{FC} curves up to T_N, thus one order of magnitude above T_g. This feature suggests the presence of a weak FM component in the system, whose ordering temperature is close to the T_N of the AF core.

This hypothesis is further strengthened by the $M(H)$ curves in Fig. 3. The hysteresis loops measured at $T = 5$, 35, and 100 K after FC ($H_{cool} = 10$ kOe) protocol shows a clear shift

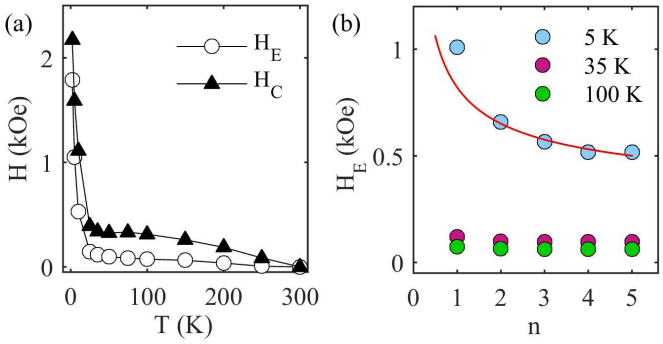

Fig. 4. (a) Temperature variation of the EB (H_E) and coercive (H_C) fields. (b) Evolution of H_E at different temperatures as a function of the number of field cycles (n). Only the $T = 5$ K curve shows training effect, which can be fitted according to the expression $H_E(n) - H_E(\infty) = k/\sqrt{n}$ (red line).

along the negative field axis, thus confirming the existence of the EB effect in the system. The temperature dependence of the EB (H_E) and coercive (H_C) fields is shown in Fig. 4(a). Although both H_E and H_C present a drastic fall above T_g, however, they persist up to T_N that determines the onset of the EB. Therefore, two well-defined regimes can be observed in the EB temperature variation. While the exchange coupling between the AF core and the SG-like shell seems to be at the origin of the EB below $T = T_g$, the question arises: what is causing the EB effect between $T_g < T < T_N$? In this respect, as commented in Section I, the boundary of an ME antiferromagnet has an equilibrium magnetization, which is coupled to the AF phase and can be switched by reversing the external magnetic field [23]. This microscopic boundary magnetization mainly appears in the case of Cr_2O_3 through a spin-canting component with respect to the AF direction and presents a monotonic decrease with T that vanishes at $T = T_N$. In other words, the same magnetic symmetry, which allows for the linear ME effect in Cr_2O_3, also enables the

explanation of both the weak FM signal and the EB effect we observe in the temperature interval $T_g < T < T_N$.

In order to discern the different nature of the EB effect occurring above and below $T = T_g$, the so-called training effect has been studied at $T = 5$, 35, and 100 K (Fig. 3). This process describes the evolution of the $M(H)$ loop when the system is successively field-cycled at a given temperature after the FC protocol. The EB effect involving the SG phase is typically due to some magnetic moments frozen at the interface during FC. Figs. 3(d) and 4(b) show that this nonequilibrium character leads to an irreversible decrease of H_E at $T = 5$ K as the magnetic field is cycled up to five times ($n = 5$). The reduction of H_E with n is satisfactorily fitted with the empirical relation, $H_E(n) - H_E(\infty) = k/\sqrt{n}$, where $H_E(\infty)$ is the value at $n \to \infty$ [28]. The red curve in Fig. 4(b) exhibits the best fit for $H_E(\infty) = 215(5)$ Oe and $k = 520(70)$ Oe. In contrast, the FC hysteresis loops measured at $T = 35$ and 100 K [Fig. 3(e) and (f)] do not exhibit any training effect [Fig. 4(b)]. This is in good agreement with previous reports on ME antiferromagnets, where the EB is an equilibrium property of the system [23].

IV. Conclusion

Highly crystalline single-domain Cr_2O_3 NPs present two well-defined temperature regimes for the ocurrence of the EB effect. On the one hand, the exchange coupling between the AF core and its uncompensated boundary magnetization gives rise to a robust EB (∼100 Oe), which persists up to the T_N (∼270 K) of the AF core and does not experience any training effect. On the other hand, the coupling between the magnetically disordered SG-like surface shell and the AF core is at the origin of a moderate EB effect (∼2000 Oe) that vanishes above ∼25 K and presents a strong decrease upon field cycling.

Acknowledgment

N.R.-M gratefully acknowledges doctoral grant FPU12/03381 from the Ministerio de Educación, Cultura y Deporte (MECD, Spain) and a mobility fellowship from the University of Oviedo Campus of Excellence-Santander Bank Program (2015). H.S. acknowledges support from the Bizkaia Talent Program, Basque Country (Spain). J.A. acknowledges the financial support provided through a postdoctoral fellowship from Basque Government. This work was financially supported by research projects MAT2014-56116-C4-2-R (MEC, Spain), FC-15-GRUPIN14-037 (Asturias Government, Spain), DE-FG02-07ER46438 (U.S. Department of Energy, Office of Basic Energy Sciences, Division of Materials Science and Engineering), 14-37427 (Grant Agency of the Czech Republic). Thanks are due to Institut Laue-Langevin (France) for allocating beam time (proposal number 5-31-2353) and to the Scientific-Technical Services of the University Oviedo for providing assistance in transmission microscopy image acquisition and magnetic measurements.

References

[1] P. Curie, "Sur la symétrie dans les phénoménes physiques, symétrie d'un champ électrique et d'un champ magnétique," *J. Phys. Theor. Appl.*, vol. 3, no. 1, pp. 393–415, 1894.
[2] L. D. Landau and E. M. Lifshitz, *Electrodynamics of Continuous Media*, vol. 8. New York, NY, USA: Pergamon, 1960.
[3] I. E. Dzyaloshinskii, "On the magneto-electrical effect in antiferromagnets," *Sov. Phys.—JETP*, vol. 10, no. 3, p. 628, 1960.
[4] B. D. H. Tellegen, "The gyrator, a new electric network element," *Philips Res. Rep.*, vol. 3, pp. 81–101, Apr. 1948.
[5] G. A. Prinz, "Device physics—Magnetoelectronics," *Science*, vol. 282, no. 5394, pp. 1660–1663, 1998.
[6] M. Gajek *et al.*, "Tunnel junctions with multiferroic barriers," *Nature Mater.*, vol. 6, pp. 296–302, Mar. 2007.
[7] W. Eerenstein, N. D. Mathur, and J. F. Scott, "Multiferroic and magnetoelectric materials," *Nature*, vol. 442, no. 7104, pp. 759–765, 2006.
[8] X. Marti *et al.*, "Room-temperature antiferromagnetic memory resistor," *Nature Mater.*, vol. 13, no. 4, p. 367, 2014.
[9] I. Fina *et al.*, "Anisotropic magnetoresistance in an antiferromagnetic semiconductor," *Nature Commun.*, vol. 5, p. 4671, Sep. 2014.
[10] R. Ramesh, "Ferroelectrics: A new spin on spintronics," *Nature Mater.*, vol. 9, pp. 380–381, May 2010.
[11] J. Nogués *et al.*, "Exchange bias in nanostructures," *Phys. Rep.*, vol. 422, no. 3, pp. 65–117, 2005.
[12] V. Skumryev *et al.*, "Magnetization reversal by electric-field decoupling of magnetic and ferroelectric domain walls in multiferroic-based heterostructures," *Phys. Rev. Lett.*, vol. 106, p. 057206, Feb. 2011.
[13] S. M. Wu, "Reversible electric control of exchange bias in a multiferroic field-effect device," *Nature Mater.*, vol. 9, pp. 756–761, Jul. 2010.
[14] J. F. Scott, "Room-temperature multiferroic magnetoelectrics," *NPG Asia Mater.*, vol. 5, p. e72, Nov. 2013.
[15] G. Catalan and J. F. Scott, "Physics and applications of bismuth ferrite," *Adv. Mater.*, vol. 21, no. 24, pp. 2463–2485, 2009.
[16] P. Borisov, A. Hochstrat, X. Chen, W. Kleemann, and C. Binek, "Magnetoelectric switching of exchange bias," *Phys. Rev. Lett.*, vol. 94, p. 117203, Mar. 2005.
[17] N. Rinaldi-Montes *et al.*, "Interplay between microstructure and magnetism in NiO nanoparticles: Breakdown of the antiferromagnetic order," *Nanoscale*, vol. 6, no. 1, p. 457, 2014.
[18] A. Punnoose, H. Magnone, M. S. Seehra, and J. Bonevich, "Bulk to nanoscale magnetism and exchange bias in CuO nanoparticles," *Phys. Rev. B*, vol. 64, p. 174420, Oct. 2001.
[19] N. Rinaldi-Montes *et al.*, "Disentangling magnetic core/shell morphologies in Co-based nanoparticles," *J. Mater. Chem. C*, vol. 4, no. 12, p. 2302, 2016.
[20] D. Tobia, E. Winkler, R. D. Zysler, M. Granada, and H. E. Troiani, "Size dependence of the magnetic properties of antiferromagnetic Cr_2O_3," *Phys. Rev. B*, vol. 78, p. 104412, Sep. 2008.
[21] R. Otero-Lorenzo, M. C. Weber, P. A. Thomas, J. Kreisel, and V. Salgueiriño, "Interplay of chemical structure and magnetic order coupling at the interface between Cr_2O_3 and Fe_3O_4 in hybrid nanocomposites," *Phys. Chem. Chem. Phys.*, vol. 16, no. 40, p. 22337, 2014.
[22] K. Trohidou, X. Zianni, and J. A. Blackman, "Surface effects on the magnetic behavior of antiferromagnetic particles," *J. Appl. Phys.*, vol. 84, no. 5, p. 2795, 1998.
[23] K. D. Belashchenko, "Equilibrium magnetization at the boundary of a magnetoelectric antiferromagnet," *Phys. Rev. Lett.*, vol. 105, p. 147204, Oct. 2010.
[24] A. B. Fuertes, "A general and low-cost synthetic route to high-surface area metal oxides through a silica xerogel template," *J. Phys. Chem. Solids*, vol. 66, no. 5, p. 741, 2005.
[25] J. Rodríguez-Carvajal, "Recent advances in magnetic structure determination by neutron powder diffraction," *Phys. B, Condens. Matter*, vol. 192, pp. 55–69, Oct. 1993.
[26] L. M. Corliss, J. M. Hastings, R. Nathans, and G. Shirane, "Magnetic structure of Cr_2O_3," *J. Appl. Phys.*, vol. 36, no. 3, p. 1099, 1965.
[27] I. V. Golosovsky *et al.*, "Magnetic phase transition in a nanostructured antiferromagnet CoO embedded in porous glass," *Phys. Solid State*, vol. 48, no. 11, pp. 2130–2133, 2006.
[28] S. Karmakar *et al.*, "Evidence of intrinsic exchange bias and its origin in spin-glass-like disordered $L_{0.5}Sr_{0.5}MnO_3$ manganites (L=Y, $Y_{0.5}Sm_{0.5}$, and $Y_{0.5}La_{0.5}$)," *Phys. Rev. B*, vol. 77, p. 144409, Apr. 2008.